

# Multi-sensor Data Fusion for Wheelchair Position Estimation with Unscented Kalman Filter

Derradji Nada<sup>1</sup> Mounir Bousbia-Salah<sup>1</sup> Maamar Bettayeb<sup>2</sup>

<sup>1</sup>LASA laboratory, Department of Electronics, Faculty of Engineering, Badji Mokhtar Annaba University, BP 12, Annaba 23000, Algeria

<sup>2</sup>Department of Electrical and Computer Engineering, College of Engineering, University of Sharjah, United Arab Emirates

**Abstract:** This paper investigates the problem of estimation of the wheelchair position in indoor environments with noisy measurements. The measuring system is based on two odometers placed on the axis of the wheels combined with a magnetic compass to determine the position and orientation. Determination of displacements is implemented by an accelerometer. Data coming from sensors are combined and used as inputs to unscented Kalman filter (UKF). Two data fusion architectures: measurement fusion (MF) and state vector fusion (SVF) are proposed to merge the available measurements. Comparative studies of these two architectures show that the MF architecture provides states estimation with relatively less uncertainty compared to SVF. However, odometers measurements determine the position with relatively high uncertainty followed by the accelerometer measurements. Therefore, fusion in the navigation system is needed. The obtained simulation results show the effectiveness of proposed architectures.

**Keywords:** Data fusion, unscented Kalman filter (UKF), measurement fusion (MF), navigation, state vector fusion (SVF), wheelchair.

## 1 Introduction

Navigation system is one of the most used applications on wheelchairs in the field of robotic systems, it can provide advantages to users of this type of chairs due to its simplicity. In ordinary life, this category needs to navigate and to know strategic places such as parking, metro stations and also inside a building composed of several places without the help of anyone. This requires the development of a system capable to accomplish these tasks, which allow the places identification and easy navigation, including helping to locate the chair mobility at any time. Practically, the location determination using a single sensor is insufficient to capture all relevant characteristics of real environments. Then, it is necessary to combine data from multiple sensors in a process known as fusion. Multi-sensor data fusion is a technology to allow combining information from several sensors, where the goal is to have a better accuracy and to give a more precise result than the one that could be obtained by the use of one single sensor<sup>[1, 2]</sup>. On the other hand, the multi-sensor data fusion techniques are applied to improve the system performance in several ways, such as increasing the robustness and reliability, and the methods are used to optimize uncertainty and to reduce the reduction time of measurement and cost<sup>[3, 4]</sup>. In the literature, a few authors have worked in this research area<sup>[5, 6]</sup>. For instance, Naidu<sup>[7]</sup> presented different fusion architectures to combine the radar data with infra-red

search and track (IRST) in the target tracking system by using extended Kalman filter (EKF). In [8], an EKF was designed. It combines the noisy data measurements of encoders (ENC), compass and accelerometer (ACC) in order to obtain the best position estimate while reducing measurement uncertainties. The proposed algorithm is based on two data fusion architectures, state vector fusion (SVF) and measurement fusion (MF). Simpson et al.<sup>[9]</sup> developed smart wheelchairs for navigation assistance mainly in indoor environments, however Ding et al.<sup>[10]</sup> developed a smart wheelchair equipped with wireless internet access and global positioning system (GPS). Defects of the previous methods are of large cost in addition to being dependent to being not effective in closed places and other places with internet access. In the network-centric applied research team (N-CART), within the NEPWAK project, Ferworn et al.<sup>[11]</sup> introduced techniques for modifying and using power wheelchairs as mobile platforms, enabling communication and remote control, and extended the mobility range of Ferworn NEPWAK beyond a local area. Whereas in [12], the authors described the development of a navigation system to give a semi-autonomous operation of wheelchairs where they make extensive use of freely available open source software. However, Wattavarangkul and Wakahara<sup>[13]</sup> present an indoor navigation system for wheelchairs, using smartphones as a sensor for navigation tools. The system in our hands is depending on a range of sensors which are different in terms of manufacturer, technology, mechanism of action and the action protocol. There exist many complications and problems in the case of mixing them<sup>[14]</sup>. For this reason, our task in this paper is to find the best way that allows the use of different information from various sensors and simultaneously make correct

Research Article  
Manuscript received July 24, 2015; accepted May 11, 2016; published online April 19, 2017  
Recommended by Associate Editor Min Cheol Lee  
© Institute of Automation, Chinese Academy of Sciences and Springer-Verlag Berlin Heidelberg 2017

judgments. In the literature, different navigation systems are reformulated as a nonlinear estimation problem where the optimal solution is given by the EKF<sup>[15]</sup>. EKF has been a popular approach for localization of a mobile robot<sup>[16]</sup>. However, the estimation quality performance of the EKF depends on the correct a priori knowledge of process measurement noise and covariance matrices  $Q$  and  $R$ , respectively. Imprecise knowledge of these statistics can lead to a significant degradation in performance. The appearance of the family of deterministic methods shows that the unscented Kalman filter (UKF) can aim higher estimation precision than EKF. Fundamental difference between EKF and UKF is on the manner in which the Gaussian random variable (GRV) is shown for propagating through the system dynamics. In the EKF, state distribution is approximated analytically, which can introduce large errors in the true covariance of GRV, this can lead to suboptimal performance and sometimes filter divergence. Nevertheless, in UKF the reconciliation of state estimated distribution is made by points construction with different weights based on deterministic methods<sup>[17]</sup>. These points are able to capture the true mean and covariance of the GRV. The problem connected with UKF resides in computational cost and numerical instability, also it is not always able to have these two properties and algorithms may diverge. The divergence in general may occur due to different reasons, including incorrect or incomplete model underlying the physical system<sup>[18]</sup>:

1) Loss of information to capture the true posterior density changes completely, for example, a nonlinear filter designed under the Gaussian assumption may fail to capture the key characteristics of a posterior density multimodal.

2) The high degree nonlinear system describing numerical errors in equations at the state space model levels.

3) Numerical errors. Indeed, each of the aforementioned filters has its own domain of applicability and it is doubtful that a single filter would be considered effective for a wide range of applications. The motivation of this study was to introduce a more accurate nonlinear filter that could be applied to solve a wide range (from low to large) nonlinear filtering problems. In this aspect, we find two architectures of multi-sensor data fusion, able to use the information from all sources and merge them to provide optimal information.

The purpose of this paper is to improve the performance of this estimator (UKF) and find architectures able to combine noisy measurements from all sources in order to obtain the best estimate of the state, while reducing measurement uncertainty. The first technique is a fusion architecture which is a measurement fusion (MF), and the second one is another architecture with different principles that is the state vector fusion (SVF)<sup>[5, 14]</sup>. The two proposed methods of fusion architectures proved their effectiveness in this area and can handle any kind of sensors. They require only a small number of sensors with the lowest cost.

This paper is organized as follows: details of the system and the fusion algorithms are respectively described in Sections 2 and 3. The study is reinforced by evaluation of

each studied method in Section 4. Section 5 presents the results of the simulation. The conclusion includes system evaluation as well as the advantages and disadvantages of the proposed algorithm.

## 2 System sensor design

The sensor system consists of a magnetic compass, an accelerometer and two odometers (absolute encoders). These odometers determine the position  $(x, y)$  and the heading using the rotary encoders<sup>[19]</sup>. Mounted on the wheel, they deliver information about elementary rotation, which by integration gives a measure of the overall motion. The resolution of the measurement of the wheels speed is increased in a ratio corresponding to that of the motion transmission system. Its accuracy depends on the sharpness of the network features, the quality of the mechanical design and the performance of the electronic signal processing (interpolation, scanning)<sup>[20]</sup>. The encoder consisted of three parts: mechanical axis, disc with its reader, and output signals. The disc has  $n$  tracks divided into  $n$  equal segments alternating opaque and transparent. A pair of optical transceivers is assigned in each track. For each position of the axis, the disc provides a code when the length  $n$  is  $(\frac{1}{2^n})$ -th rounds. We have chosen a simple absolute encoder ( $2^{11} = 2048$  points) of 64 laps. The odometers are based on simple equations that are verified when the wheel revolutions can be translated precisely into linear displacements relative to the earth<sup>[21]</sup>. In the case of wheel slippage or other more subtle causes, the wheel laps cannot translate the linear movement proportionally. The resulting errors can be classified into two groups: systematic and unsystematic. Systematic errors are those resulting from the kinematic imperfections of the vehicle, such as unequal wheel diameters or uncertainty about the exact wheel-base. On the other hand, unsystematic errors are those resulting from the road interaction with wheels like the dents or the cracks<sup>[20]</sup>. Many solutions have been proposed to improve the systematic errors. Decoders must be put on special wheels which are not subject to the vehicle load effects, and can be matched to the drive wheels. Unsystematic errors are corrected by the inclusion of other types of sensors. The orientation of wheelchair is determined by using a magnetic compass HMC1002, also called a magnetometer which indicates the direction of magnetic north<sup>[22]</sup>. Generally, magnetic declination is compensated, so that the sensor delivers continuously an absolute measure of heading related to the direction of true north. The module has two axes  $X$  and  $Y$ , based on the Hall effect with the resolution of  $0.1^\circ$  as in [23]. In order to achieve the degree of compass accuracy, a magnetic sensor is needed to reliably solve the angular variations of  $0.1^\circ$  using the following relationship of orientation<sup>[24]</sup>:

$$\theta = \tan^{-1}\left(\frac{y}{x}\right). \quad (1)$$

To take account of the tangent function validity over 180° and to not allow calculation involving division by 0, the following equations can be used:

$$\theta = \begin{cases} 90^\circ, & x = 0 \text{ and } y < 0 \\ 270^\circ, & x = 0 \text{ and } y > 0 \\ \left( \left( 180 - \tan^{-1}\left(\frac{y}{x}\right) \times \frac{180}{\pi} \right)^\circ, & x < 0 \\ \left( \left( -\tan^{-1}\left(\frac{y}{x}\right) \times \frac{180}{\pi} \right)^\circ, & x > 0 \text{ and } y < 0 \\ \left( \left( 360 - \tan^{-1}\left(\frac{y}{x}\right) \times \frac{180}{\pi} \right)^\circ, & x > 0 \text{ and } y > 0. \end{cases} \quad (2)$$

To measure the linear acceleration, an accelerometer is used. The principle of most accelerometers is based on the fundamental law of motion which is  $F = m \times a$ , where  $F$  is the force (N),  $m$  is the mass (kg) and  $a$  is the acceleration ( $m/s^2$ ). Specifically, it consists of the equality between the inertial mass of the seismic force sensor and a biasing force applied to the mass. One thing in common for all accelerometers is that the displacement of the seismic mass will be measured by a position measurement interface circuit and it is then converted to a type of signal<sup>[25–27]</sup>. In our study, it is assumed that the measurement interface provides two outputs  $x$  and  $y$ .

### 3 Algorithms for estimation and multi-sensor data fusion

#### 3.1 Kinematics model design

The proposed platform occupies the wheelchair with three sensor types, compass, accelerometer, and absolute encoders having the ability to perceive parameters helping to determine the position. The raw data of these sensors are combined using an unscented Kalman filter. The objective is then to determine the position of the wheelchair during operations as accurately as possible<sup>[21]</sup>.

We start with the kinematic model of the wheelchair. On each rear wheel, an odometer is mounted. The measurements are made by rotary encoders coupled to the wheel axis. Fig. 1 shows the system coordinates as well as the wheelchair notations where  $(X_r, Y_r)$  are the global coordinates and  $(X_f, Y_f)$  are the local coordinates of the wheelchair frame.  $r$  denotes the radius of the wheel and  $l$  the distance between the two wheels. During a sampling period  $\Delta t$ <sup>[28, 29]</sup>, left and right rotational speeds  $v_g$  and  $v_d$  create elementary displacements  $\Delta d_g$  and  $\Delta d_d$  which are driven respectively by left and right wheels as in (3):

$$\begin{cases} \Delta d_g = \Delta t \times r \times v_g \\ \Delta d_d = \Delta t \times r \times v_d. \end{cases} \quad (3)$$

These can be converted to linear incremental movement  $\Delta d$  of the chair frame center and the orientation angle  $\Delta \theta$  as

in (4):

$$\begin{cases} \Delta d = \frac{(\Delta d_g + \Delta d_d)}{2} \\ \Delta \theta = \frac{(\Delta d_g - \Delta d_d)}{l}. \end{cases} \quad (4)$$

According to [27, 28], the basic movements during time  $k$  to  $k + 1$  are given by the following equation:

$$\begin{cases} x_{k+1} = x_k + \Delta d_k \times \cos(\Phi) \\ y_{k+1} = y_k + \Delta d_k \times \sin(\Phi) \\ \theta_{k+1} = \theta_k + \Delta \theta_k \end{cases} \quad (5)$$

where  $\Phi = (\theta_k + \frac{\Delta \theta_k}{2})$ .

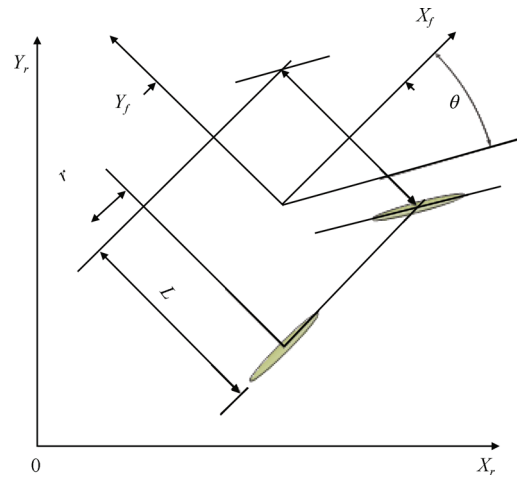


Fig. 1. Configuration and measurement model. System is equipped with both encoders, compass and accelerometer

Practically, (5) is not really accurate because inevitable errors occur in the system. These errors can be both systematic such as the imperfect model and unsystematic such as wheel slippage. They have accumulated characteristics that affect the system stability if adequate compensation is not considered. In our system, the compensation is performed by merging measures of a compass, an accelerometer and absolute encoders. This is accomplished by using the UKF. Equation (6) is described by a nonlinear function  $f$ , coordinate of a wheelchair and a process of Gaussian noise  $w$ . The state of the system can be observed by some absolute measures that can be described by a nonlinear function  $h$ , coordinate of a wheelchair and an independent Gaussian noise process  $v$ . The system is described as

$$\begin{cases} X_{k+1} = f(X_k, u_k, w_k) \\ Z_k = h(X_k, v_k) \end{cases} \quad (6)$$

where  $X_k$  is the state vector at time  $k$  and  $Z_k$  is the observation vector at time  $k$ .

The random variables  $w_k$  and  $v_k$  represent the process and measurement noise respectively. They are assumed to be independent from each other, white, and with normal probability distributions:

$$w_k \sim N(0, Q_k), v_k \sim N(0, R_k), E(w_i v_j^T) = 0.$$

In the case of the nonlinear model, the optimal estimation solution is the EKF. This method of filtering gives good results when the models of evolution of the status and measurement are close to the linear case (first order approximation). However, the optimality of the filter and the convergence are not guaranteed. It can be linearized only in the case of existence of the Jacobian matrix that can be difficult to calculate and may generate errors in the algorithm. In this work, the deterministic methods that share the same principles are studied. These filters are based on a deterministic sampling approach for the Bayesian solution numerically, using the unscented transformation for obtaining the unscented Kalman filter (UKF)<sup>[30]</sup>.

### 3.2 Unscented transformation (UT)

Unscented transformation (UT) is a method for calculating the statistics of a random variable which undergoes a nonlinear transformation. The UT builds on the principle that it is easier to approximate a probability distribution of an arbitrary nonlinear function. The UT uses a small number of chosen test points, which are called Sigma points. Each sigma point is propagated through the nonlinear function, and then the mean and covariance are computed through the use of a weighted statistical linear regression process<sup>[31]</sup>. These points are then propagated through the nonlinear function whose mean and covariance of the estimation are then recovered. The result is a filter that captures most accurate mean and the true covariance<sup>[32]</sup>.

### 3.3 Unscented Kalman filter (UKF)

For the  $n$ -dimensional random variable with known mean and covariance  $P_x$ , a given known nonlinear transformation  $y = h_{NL}(X)$ , the mean and covariance of  $y$ , denoted as  $y$  and  $P_y$  can be estimated from  $2L + 1$  sigma point vectors as follows<sup>[33]</sup>:

$$\begin{cases} X_0 = \bar{X}, & i = 0 \\ X_i = \bar{X} + \left[ \sqrt{(L + \lambda) P_x} \right]_i, & i = 1 \dots L \\ X_i = \bar{X} - \left[ \sqrt{(L + \lambda) P_x} \right]_{i-n_x}, & i = L + 1 \dots 2L \end{cases} \quad (7)$$

where  $\left[ \sqrt{(n_x + \lambda) P_x} \right]_i$  is the  $i$ -th column of the matrix square root of  $(L + \lambda) P_x$ ,  $i$  is an index of sigma points,  $L$  is the dimension number of the augmented state vector,  $\lambda$  is computed by  $\lambda = \alpha^2 (L + k) - L$ , with  $\alpha$  and  $k$  are scaling parameters that determine how far the sigma points are spread from the mean  $\bar{X}$ . In this paper,  $\alpha = 10^{-3}$ ,  $k = 0$  and  $B = 2$ . The weight is defined as

$$\begin{cases} W_{0(X)} = \frac{\lambda}{n_x + \lambda}, & i = 0 \\ W_{0(P)} = \frac{\lambda}{n_x + \lambda} + (1 - \alpha^2 + \beta), & i = 0 \\ W_{i(X)} = W_{i(P)} = \frac{1}{2(n_x + \lambda)}, & i = 1 \dots 2L. \end{cases} \quad (8)$$

UKF algorithm proceeds according to the following successive stages<sup>[17]</sup>: We assume that the observations denoted as

$y_k$ , state noise and observation are  $Q$  and  $R$ . The initial state and initial covariance are  $X_0$  and  $P_0$ .

1) Initialisation

$X_{0|0} = X_0, P_{0|0} = P_0$ . Compute the weight  $W_i$ , refer to (8).

2) Estimation

For  $k = 1$  to infinity

a) Prediction

i) Calculate  $X_i$  deterministic samples according to (7):

$$(X_0, X_1, \dots, X_L, \dots, X_{2L}).$$

ii) Evaluation of samples propagates

$(\hat{X}_{0,k|k-1}, \dots, \hat{X}_{n_x,k|k-1}, \dots, \hat{X}_{2n_x,k|k-1})$  such that

$$\hat{X}_{i,k|k-1} = f(X_{i,k-1|k-1}, u_{k-1}). \quad (9)$$

iii) The predicted state and the predicted covariance are computed as

$$X_{k|k-1} = \sum_{i=0}^{2L} w_{i(x)} \hat{X}_{i,k|k-1} \quad (10)$$

$$P_{k|k-1} \approx \sum_{i=0}^{2L} w_{i(p)} (\hat{X}_{i,k|k-1} - X_{k|k-1}) \times (\hat{X}_{i,k|k-1} - X_{k|k-1})^T + Q_k \quad (11)$$

where

$$Q_k = \begin{bmatrix} \sigma_x^2 & 0 & 0 \\ 0 & \sigma_y^2 & 0 \\ 0 & 0 & \sigma_\theta^2 \end{bmatrix}. \quad (12)$$

b) Correction

i) Correct and propagate evaluation samples

$$(\hat{Y}_{0,k|k-1}, \dots, \hat{Y}_{L,k|k-1}, \dots, \hat{Y}_{2L,k|k-1}) \quad (13)$$

knowing that

$$\hat{Y}_{i,k|k-1} = h(\hat{X}_{i,k|k-1}, u_k). \quad (14)$$

ii) Estimate the predicted observation  $\hat{y}_{k|k-1}$ , the predicted covariance error  $P_{yy,k|k-1}$  and the cross covariance  $P_{xy,k|k-1}$

$$\hat{y}_{k|k-1} = \sum_{i=0}^{2L} w_{i(x)} \hat{Y}_{i,k|k-1} \quad (15)$$

$$P_{yy,k|k-1} = \sum_{i=0}^{2L} w_{i(p)} (\hat{Y}_{i,k|k-1} - \hat{y}_{k|k-1}) \times (\hat{Y}_{i,k|k-1} - \hat{y}_{k|k-1})^T + R \quad (16)$$

$$P_{xy,k|k-1} = \sum_{i=0}^{2L} w_{i(p)} (\hat{X}_{i,k|k-1} - X_{k|k-1}) \times (\hat{Y}_{i,k|k-1} - \hat{y}_{k|k-1})^T. \quad (17)$$

iii) Compute the Kalman gain  $G_k$ :

$$G_k = \frac{P_{xy,k|k-1}}{P_{yy,k|k-1}} \tag{18}$$

iv) Correct the state and the covariance matrix error:

$$X_{k|k} = X_{k|k-1} + G_k (y_k - \hat{y}_{k|k-1}) \tag{19}$$

$$P_{k|k} = P_{k|k-1} - G_k P_{yy,k|k-1} G_k^T \tag{20}$$

End for.

### 3.4 Multi-sensor data fusion

To improve the measurement performance, we have proposed two architectures to merge the sensors measures state vector fusion (SVF) and measurement fusion (MF). In both architectures, we used compass measures merged with the accelerometer measurements in a single measurement vector,  $Y_k^{(b)} = [x_a y_a \theta_b]^T$ .

The covariance matrix of this vector is defined as follows:

$$R^{(b)} = \begin{bmatrix} \sigma_{a,x}^2 & 0 & 0 \\ 0 & \sigma_{a,y}^2 & 0 \\ 0 & 0 & \sigma_{b,\theta}^2 \end{bmatrix} \tag{21}$$

where  $Y_k^{(c)} = [x_c y_c \theta_b]^T$  vector corresponds to the odometer measurements merged with the compass measurements. The covariance matrix of this vector is defined as

$$R^{(c)} = \begin{bmatrix} \sigma_{c,x}^2 & 0 & 0 \\ 0 & \sigma_{c,y}^2 & 0 \\ 0 & 0 & \sigma_{b,\theta}^2 \end{bmatrix} \tag{22}$$

#### 3.4.1 SVF architecture (state vector fusion)

The operation principle of SVF is based on the position calculation from the measurement of each sensor separately and the resulting state vectors are merged to obtain a final state vector. The covariance matrices are combined to give the final state matrix (Fig. 2).

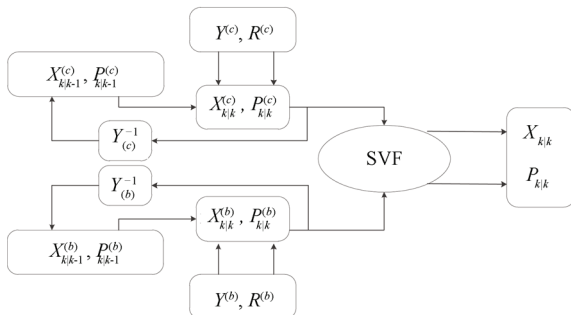


Fig. 2 Diagram of SVF architecture

For measurements of  $Y_k^{(c)}$ :

1) Prediction stage:

$$\hat{X}_{i,k|k-1}^{(c)} = f(X_{i,k-1|k-1}^{(c)}, u_{k-1}) \tag{23}$$

$$X_{k|k-1}^{(c)} = \sum_{i=0}^{2L} w_{i(x)} \hat{X}_{i,k|k-1}^{(c)} \tag{24}$$

$$P_{k|k-1}^{(c)} = \sum_{i=0}^{2L} w_{i(p)} (\hat{X}_{i,k|k-1}^{(c)} - X_{k|k-1}^{(c)}) \times (\hat{X}_{i,k|k-1}^{(c)} - X_{k|k-1}^{(c)})^T + Q_k \tag{25}$$

2) Correction stage:

$$\hat{y}_{i,k|k-1}^{(c)} = h(\hat{X}_{i,k|k-1}^{(c)}, u_k) \tag{26}$$

$$\hat{y}_{k|k-1}^{(c)} = \sum_{i=0}^{2L} w_{i(x)} \hat{y}_{i,k|k-1}^{(c)} \tag{27}$$

$$P_{yy,k|k-1}^{(c)} = \sum_{i=0}^{2L} w_{i(p)} (\hat{Y}_{i,k|k-1}^{(c)} - \hat{y}_{k|k-1}^{(c)}) \times (\hat{Y}_{i,k|k-1}^{(c)} - \hat{y}_{k|k-1}^{(c)})^T + R^{(c)} \tag{28}$$

$$P_{xy,k|k-1}^{(c)} = \sum_{i=0}^{2L} w_{i(p)} (\hat{X}_{i,k|k-1}^{(c)} - X_{k|k-1}^{(c)}) \times (\hat{Y}_{i,k|k-1}^{(c)} - \hat{y}_{k|k-1}^{(c)})^T \tag{29}$$

$$G_k^{(c)} = \frac{P_{xy,k|k-1}^{(c)}}{P_{yy,k|k-1}^{(c)}} \tag{30}$$

$$X_{k|k}^{(c)} = X_{k|k-1}^{(c)} + G_k^{(c)} (Y_k^{(c)} - \hat{y}_{k|k-1}^{(c)}) \tag{31}$$

$$P_{k|k}^{(c)} = P_{k|k-1}^{(c)} - G_k^{(c)} P_{yy,k|k-1}^{(c)} G_k^{(c)T} \tag{32}$$

For measurements of  $Y_k^{(b)}$ :

1) Prediction stage: Equations (23)–(25).

2) Correction stage: Equations (26)–(28).

SVF:

$$X_{f,k|k} = X_{k|k}^{(c)} + P_{k|k}^{(c)} \times [P_{k|k}^{(c)} + P_{k|k}^{(b)}]^{-1} \times (X_{k|k}^{(b)} - X_{k|k}^{(c)}) \tag{33}$$

$$P_{f,k|k} = P_{k|k}^{(c)} + P_{k|k}^{(b)} \times (P_{k|k}^{(c)} + P_{k|k}^{(b)})^{-1} \times P_{k|k}^{(c)T} \tag{34}$$

#### 3.4.2 MF architecture (measurement fusion)

In this architecture (Fig. 3), all sources of measurements are merged into a measurement vector. On the other hand, the covariance matrices of these sources are also merged to produce the same results.

1) Prediction stage:

$$\hat{X}_{i,k|k-1} = f(X_{i,k-1|k-1}, u_{k-1}) \tag{35}$$

$$X_{k|k-1} = \sum_{i=0}^{2L} w_{i(x)} \hat{X}_{i,k|k-1} \tag{36}$$

$$P_{k|k-1} = \sum_{i=0}^{2L} w_{i(p)} (\hat{X}_{i,k|k-1} - X_{k|k-1}) \times (\hat{X}_{i,k|k-1} - X_{k|k-1})^T + W_k \times Q_{k-1} \times W_k^T \tag{37}$$

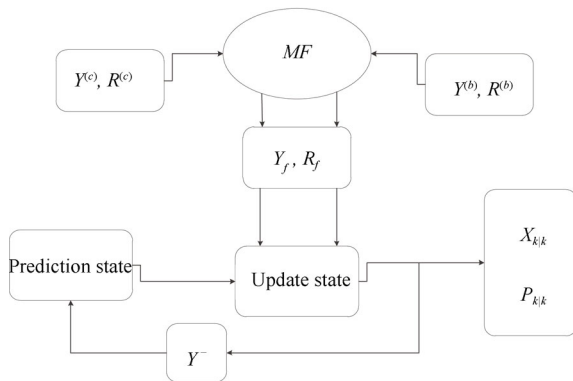


Fig. 3 Diagram of MF architecture

2) MF:

$$Y_f = Y^{(c)} + Y^{(c)} \times [R^{(c)} + R^{(b)}]^{-1} \times (Y^{(b)} - Y^{(c)}) \quad (38)$$

$$R_f = R^{(c)} - R^{(c)} \times [R^{(c)} + R^{(b)}]^{-1} \times R^{(c)}. \quad (39)$$

3) Correction stage:

$$\hat{Y}_{i,k|k-1} = h(\hat{X}_{i,k|k-1}, u_k) \quad (40)$$

$$\hat{y}_{k|k-1} = \sum_{i=0}^{2L} w_{i(x)} \hat{Y}_{i,k|k-1} \quad (41)$$

$$P_{yy,k|k-1} = \sum_{i=0}^{2L} w_{i(p)} (\hat{Y}_{i,k|k-1} - \hat{y}_{k|k-1}) \times (\hat{Y}_{i,k|k-1} - \hat{y}_{k|k-1})^T + R_f \quad (42)$$

$$P_{xy,k|k-1} = \sum_{i=0}^{2L} w_{i(p)} (\hat{X}_{i,k|k-1} - X_{k|k-1}) \times (\hat{Y}_{i,k|k-1} - \hat{y}_{k|k-1})^T \quad (43)$$

$$G_k = \frac{P_{xy,k|k-1}}{P_{yy,k|k-1}} \quad (44)$$

$$X_{k|k} = X_{k|k-1} + G_k (Y_f - \hat{y}_{k|k-1}) \quad (45)$$

$$P_{k|k} = P_{k|k-1} - G_k P_{yy,k|k-1} G_k^T. \quad (46)$$

### 4 Performance evaluation of the two algorithms

Both fusion architectures are evaluated by computing the following performance metrics:

1) Absolute error (AE) in  $x$  positions is

$$AE_x = |x_i - \hat{x}_i|, \quad i = 1, 2, \dots, N \quad (47)$$

similarly for  $y$  positions and  $\theta$  orientation.

Where  $x_i, y_i, \theta_i$  are the true positions and  $\hat{x}_i, \hat{y}_i, \hat{\theta}_i$  are the estimated  $x_i, y_i$  positions and  $\theta_i$  orientations.

2) Mean absolute error in  $x$  positions is

$$MAE_x = \frac{1}{N} \sum_{i=1}^N |x_i - \hat{x}_i| \quad (48)$$

similarly for  $y$  positions and  $\theta$  orientation.

3) The percentage fit error (PFE) in  $x$  positions is

$$PFE_x = 100 \times \frac{norm(x - \hat{x})}{norm(x)} \quad (49)$$

similarly for  $y$  positions and  $\theta$  orientation.

4) Root mean square error in  $x$  and  $y$  position is

$$RMSPE = \sqrt{\frac{1}{N} \sum_{i=1}^N \frac{(x - \hat{x})^2 + (y - \hat{y})^2}{2}}. \quad (50)$$

5) Root sum square error in  $x$  and  $y$  positions:

$$RSSPE = \sqrt{(x - \hat{x})^2 + (y - \hat{y})^2}. \quad (51)$$

6) State error (SE) is

$$SE_x = (x - \hat{x})$$

with theoretical bounds of

$$\pm 2\sqrt{\hat{P}_x}$$

$$SE_y = (y - \hat{y})$$

with theoretical bounds of

$$\pm 2\sqrt{\hat{P}_y}$$

$$SE_\theta = (\theta - \hat{\theta})$$

with theoretical bounds of

$$\pm 2\sqrt{\hat{P}_\theta}.$$

7) Compute innovation sequence  $IS = Z_k - \tilde{Z}_{k|k-1}$  while the measurements are available in Cartesian coordinates:

$$IS_x \text{ with theoretical bounds of } \pm 2\sqrt{\hat{S}_x}$$

$$IS_y \text{ with theoretical bounds of } \pm 2\sqrt{\hat{S}_y}.$$

### 5 Simulation and results

In this section, an experiment was simulated to calculate the position under two different scenarios: with the MF algorithm and the SVF algorithm.

The simulation uses the following parameters:

1) Sampling period  $\Delta t = 0.1$  s.

2) Initial state vector:  $X_0 = \begin{bmatrix} 0 & 0 & 0 \end{bmatrix}^T$ .

3) The initial covariance matrix is defined by

$$P_0 = \begin{bmatrix} 0.01 & 0 & 0 \\ 0 & 0.01 & 0 \\ 0 & 0 & 0.3 \end{bmatrix}. \quad (52)$$

Table 1 Percentage fit errors in position

ALG	PFE <sub>x</sub>	PFE <sub>y</sub>	PFE <sub>θ</sub>	RMSPE (m)
SVF	29.807 8	104.849 7	<b>52.928 5</b>	0.008 6
MF	<b>24.094 8</b>	<b>53.188 6</b>	56.024 7	<b>0.005 6</b>
ENC	68.654 1	8 964.104 0	332.756 5	0.663 7
ACC	32.990 0	56.563 6	61.320 4	0.006 1

4) The covariance matrices of measurements noise:

$$R_b = \begin{bmatrix} 10^{-8} & 0 & 0 \\ 0 & 10^{-8} & 0 \\ 0 & 0 & 85 \times 10^{-9} \end{bmatrix} \quad (53)$$

$$R_c = \begin{bmatrix} 10^{-8} & 0 & 0 \\ 0 & 10^{-8} & 0 \\ 0 & 0 & 8 \times 10^{-4} \end{bmatrix} \quad (54)$$

5) The noise system covariance matrix is

$$Q_k = \begin{bmatrix} 0.01^2 & 0 & 0 \\ 0 & 0.01^2 & 0 \\ 0 & 0 & 0.1^2 \end{bmatrix} \quad (55)$$

Both data fusion architectures are evaluated by using a sequential simulation algorithm of the unscented Kalman filter. The mean absolute error in position is shown in Table 2 and Figs. 4–7.

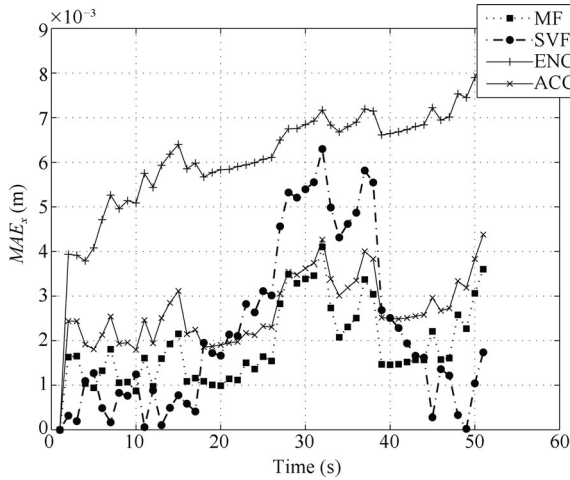


Fig. 4 Mean absolute errors in x

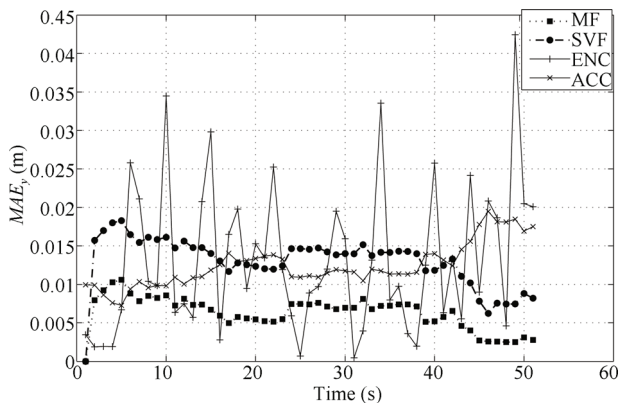


Fig. 5 Mean absolute errors in y

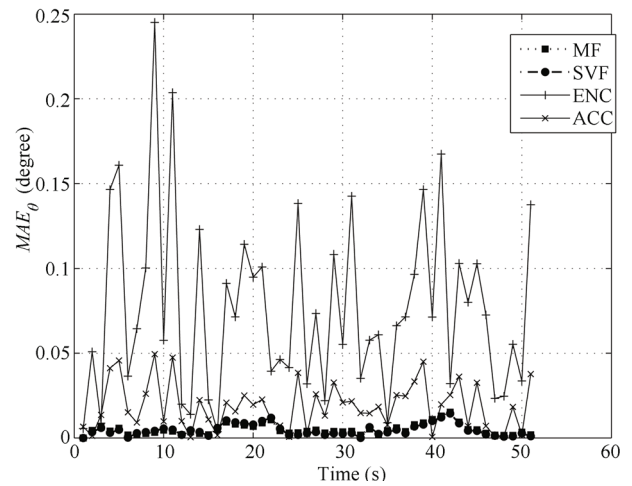


Fig. 6 Mean absolute errors in θ

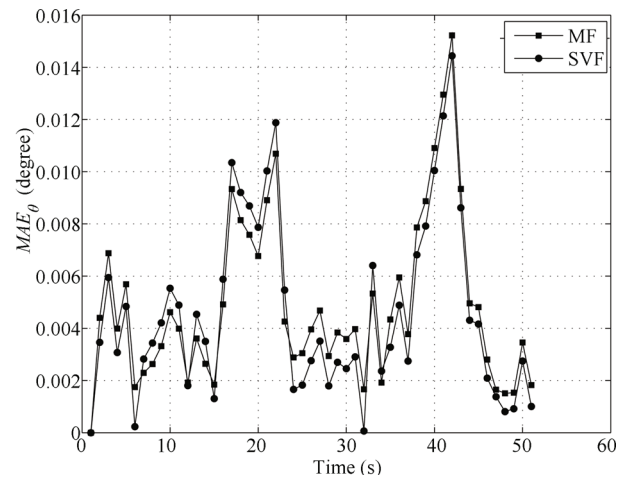


Fig. 7 Zoomed view of Fig. 6

Percentage of fit error (PFE) and the root mean square error in position (RMSPE) are presented in Table 1. The variations in the mean square error and the execution time for each algorithm are shown in Table 3 and Fig. 8.

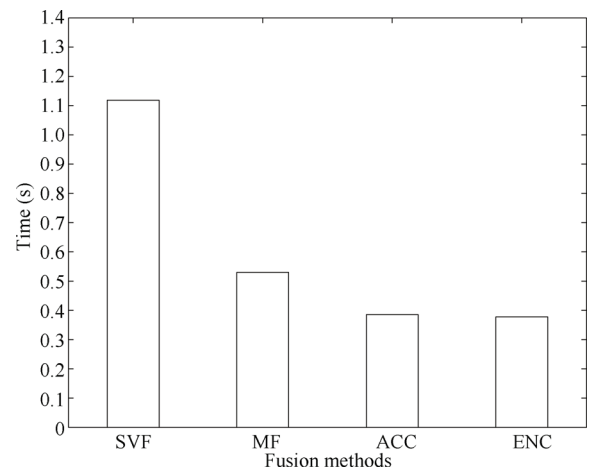


Fig. 8 Execution time for each algorithm

Table 2 Mean absolute error in position

ALG	MAE <sub>x</sub> (m)	MAE <sub>y</sub> (m)	MAE <sub>θ</sub> (degree)
SVF	0.0022	0.0129	<b>0.0046</b>
MF	<b>0.0019</b>	<b>0.0063</b>	0.0049
ENC	0.0061	1.1213	0.0341
ACC	0.0027	0.0067	0.0054

Table 3 Mean root sum variance in position and execution time

Algorithm	MRSvarP(m)	Time (s)
SVF	<b>0.0086</b>	1.9587
MF	0.0090	2.6505
ENC	0.5430	<b>0.7599</b>
ACC	0.0087	0.7703

The state error with its theoretical limits shows the filter robustness. Figs. 9 and 10 show that the MF algorithm is more robust than the SVF one and therefore presents a relatively high performance.

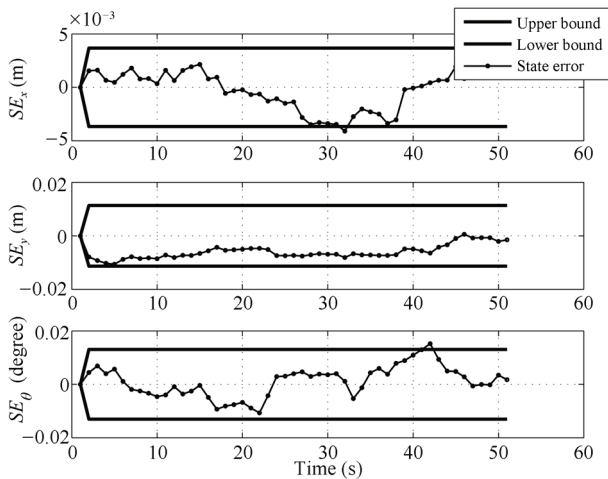


Fig. 9 State error in positions with theoretical bounds for MF algorithm

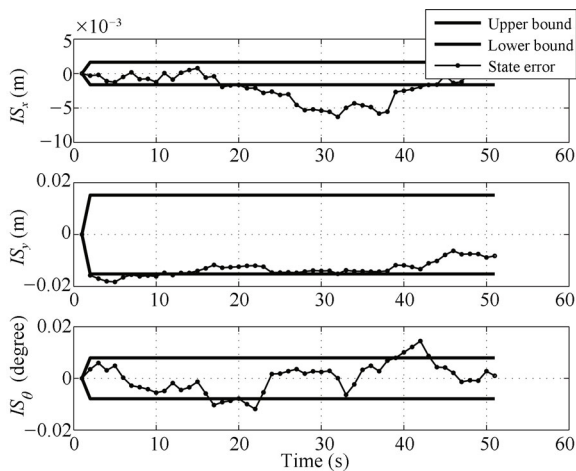


Fig. 10 State error in positions with theoretical bounds for SVF algorithm

Bold values indicate the best results. The root sum square error in position is shown in Fig. 11. From the tables and figures, we can see that the location with the odometer or accelerometer shows performance degradation compared to fusion architectures. MF shows the lowest uncertainty followed by SVF. The uncertainty in the state estimate is high if the odometer is followed by the accelerometer. This shows the need for fusion. For the execution time, localization with odometer takes less time with degraded performance.

On the other hand, we investigated the consistency of the MF and SVF algorithms using sequences of innovation with theoretical limits, as shown in Figs. 12 and 13. The simulation results show that the two algorithms are consistent.

Finally, we studied the autocorrelation (AC) of the innovation sequence to show that the two algorithms extracted all the information represented by the signal. The simulation result shows in Figs. 14 and 15 that both algorithms are satisfactory.

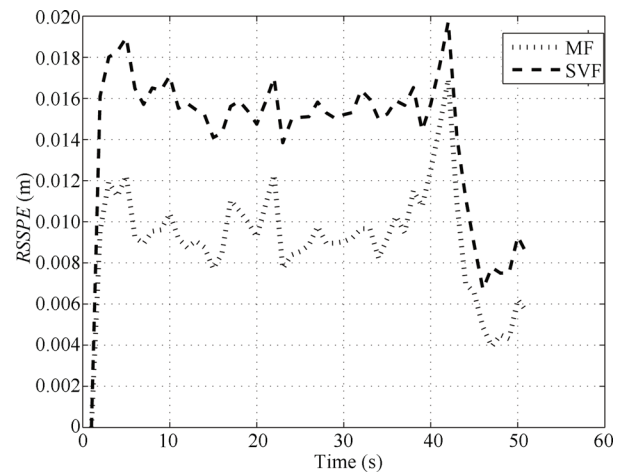


Fig. 11 Root sum square error in position

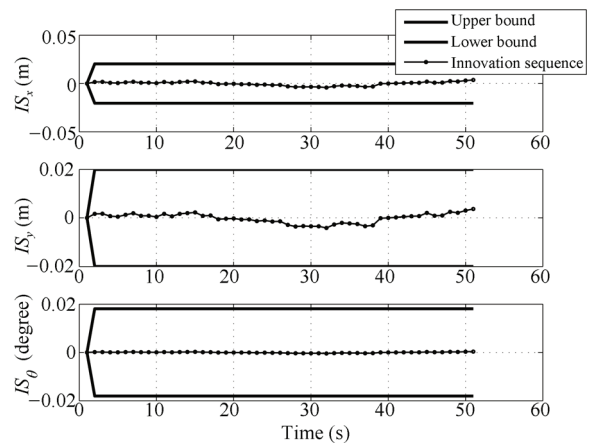


Fig. 12 Innovation sequence with theoretical bounds for MF algorithm



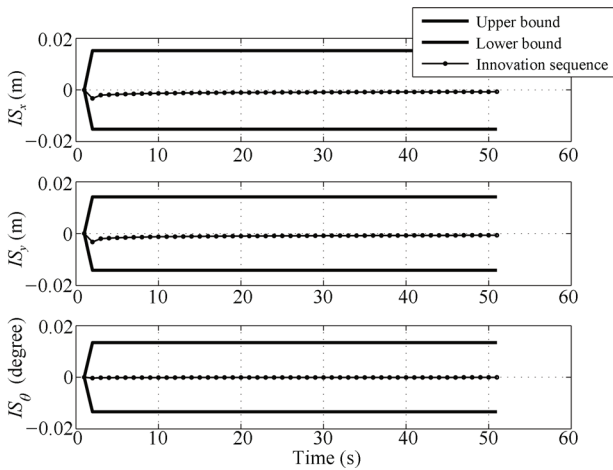


Fig. 13 Innovation sequence with theoretical bounds for SVF algorithm

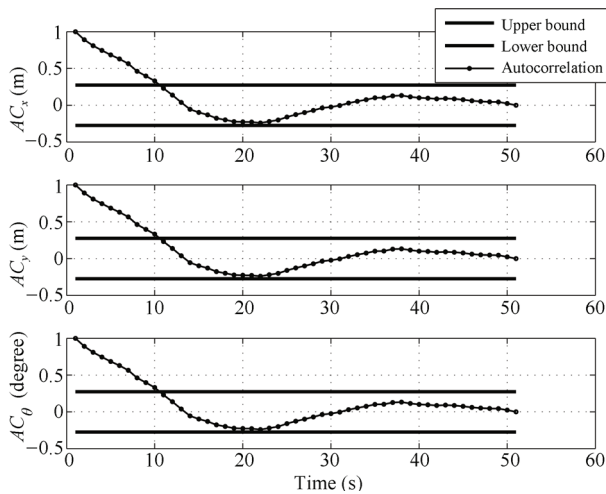


Fig. 14 Autocorrelation of innovation sequence along with theoretical bounds for MF algorithm

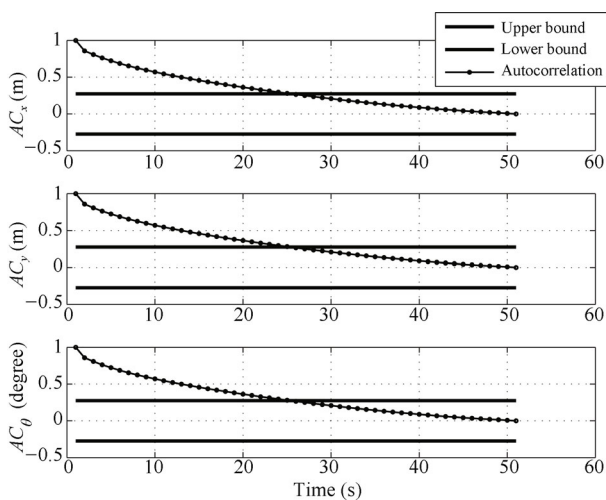


Fig. 15 Autocorrelation of innovation sequence along with theoretical bounds for SVF algorithm

## 6 Conclusions

In order to increase the UKF algorithm performance for the position estimation, we showed the importance and the need for data fusion. Two fusion algorithms (SVF and MF) were addressed and detailed mathematical expressions are given which could be useful for the implementation. The simulation results show that the MF algorithm provides state estimates with relatively less uncertainty followed by the SVF algorithm. For future development, the estimation problem of wheelchair position could also be investigated by using the cubature Kalman filter (CKF)<sup>[34]</sup>. In addition, the Bayesian nonlinear filtering using quadrature and cubature rules<sup>[35]</sup>, will also solve this problem. We hope that this work will be an effective solution for reducing navigation problems for wheelchair users.

## Acknowledgement

We would like to thank the Laboratory of Automatics and Signals at Annaba (LASA) whose members displayed great interest and support to carry out this work.

## References

- [1] S. Safari, F. Shabani, D. Simon. Multirate multisensor data fusion for linear systems using Kalman filters and a neural network. *Aerospace Science and Technology*, vol. 39, pp. 465–471, 2014.
- [2] F. Cappello, R. Sabatini, S. Ramasamy. Multi-sensor Data Fusion Techniques for RPAS Detect, Track and Avoid, SAE Technical Paper 2015-01-2475, Seattle, Washington, USA, 2015.
- [3] D. U. Guanglong, P. Zhang. Human-manipulator interface using hybrid sensors with Kalman filters and adaptive multi-space transformation. *Measurement*, vol. 55, pp. 413–422, 2014.
- [4] W. J. Qi, P. Zhang, Z. L. Deng. Robust weighted fusion Kalman filters for multisensor time-varying systems with uncertain noise variances. *Signal Processing*, vol. 99, pp. 185–200, 2014.
- [5] J. R. Raol. *Multi-Sensor Data Fusion with MATLAB®*, Boca Raton, USA: CRC Press Inc., 2009.
- [6] D. L. Hall, S. A. H. McMullen. *Mathematical Techniques in Multisensor Data Fusion*, Norwood, USA: Artech House, 2004.
- [7] V. Naidu. Fusion architectures for 3D target tracking using IRST and radar measurements. *Journal of Aerospace Sciences & Technologies*, vol. 62, no. 3, pp. 183–195, 2010.
- [8] D. Nada, M. Bousbia Salah, M. Bettayeb. Fusion architectures with extended Kalman Filter for locate wheelchair position using sensors measurements. In *Proceedings of International Conference on Electrical Sciences and Technologies in Maghreb (CISTEM)*, IEEE, Tunis, Tunisia, pp. 1–7, 2014.

- [9] R. Simpson, E. LoPresti, S. Hayashi, I. Nourbakhsh, D. Miller. The smart wheelchair component system. *The Journal of Rehabilitation Research and Development*, vol. 41, no. 3B, pp. 429–442, 2004.
- [10] D. Ding, B. Parmanto, H. A. Karimi, D. Roongpiboonsopit, G. Pramana, T. Conahan, P. Kasemsuppakorn. Design considerations for a personalized wheelchair navigation system. In *Proceedings of the 29th Annual International Conference of the IEEE Engineering in Medicine and Biology Society*, IEEE, Lyon, France, pp. 4790–4793, 2007.
- [11] A. Ferworn, A. Arora, M. Jaseemuddin. IP mobility issues for a mobile tele-robotic system-NEPWAK. *International Journal of Automation and Computing*, vol. 1, no. 1, pp. 10–16, 2004.
- [12] R. Tang, X. Q. Chen, M. Hayes, I. Palmer. Development of a navigation system for semiautonomous operation of wheelchairs. In *Proceedings of IEEE/ASME International Conference on Mechatronics and Embedded Systems and Applications (MESA)*, IEEE, Suzhou, China, pp. 257–262, 2012.
- [13] N. Wattanavarangkul, T. Wakahara. Indoor navigation system for wheelchair using smartphones. *Information Technology Convergence, Lecture Notes in Electrical Engineering*, J. J. Park, L. Barolli, F. Khafa, H. Y. Jeong, Eds., Netherlands: Springer, pp. 233–241, 2013.
- [14] J. B. Gao, C. J. Harris. Some remarks on Kalman filters for the multisensor fusion. *Information Fusion*, vol. 3, no. 3, pp. 191–201, 2002.
- [15] B. D. O. Anderson, J. B. Moore, M. Eslami. Optimal filtering. *IEEE Transactions on Systems, Man, and Cybernetics*, vol. 12, no. 2, pp. 235–236, 1982.
- [16] H. Zhao, Z. Y. Wang. Motion measurement using inertial sensors, ultrasonic sensors, and magnetometers with extended Kalman filter for data fusion. *IEEE Sensors Journal*, vol. 12, no. 5, pp. 943–953, 2012.
- [17] E. A. Wan, R. Van Der Merwe. The unscented Kalman filter. *Kalman Filtering and Neural Networks*, S. Haykin, Ed., New York, USA: John Wiley Sons Inc., pp. 221–280, 2001.
- [18] W. L. Li, S. H. Sun, Y. M. Jia, J. P. Du. Robust unscented Kalman filter with adaptation of process and measurement noise covariances. *Digital Signal Processing*, vol. 48, pp. 93–103, 2016.
- [19] S. Kernbach. Encoder-free odometric system for autonomous microrobots. *Mechatronics*, vol. 22, no. 6, pp. 870–880, 2012.
- [20] S. G. Tzafestas. 4-Mobile robot sensors. *Introduction to Mobile Robot Control*, S. G. Tzafestas, Ed., Oxford, UK: Elsevier, pp. 101–135, 2014.
- [21] S. B. Lazarus, I. Ashokaraj, A. Tsourdos, R. Zbikowski, P. M. G. Silson, N. Aouf, B. A. White. Vehicle localization using sensors data fusion via integration of covariance intersection and interval analysis. *IEEE Sensors Journal*, vol. 7, no. 9, pp. 1302–1314, 2007.
- [22] T. Guilford, G. K. Taylor. The sun compass revisited. *Animal Behaviour*, vol. 97, pp. 135–143, 2014.
- [23] Datasheet. *1-Axis and 2-Axis Magnetic Sensors HMC1001/1002/1021/-1022*, Honeywell, Morristown, USA, [Online], Available: <https://aerocontent.honeywell.com/aero/common/documents/myaerospacecatalog-documents/Missiles-Munitions/>, August 2008.
- [24] M. J. Caruso. Applications of magnetic sensors for low cost compass systems. In *Proceedings of the Position Location and Navigation Symposium*, IEEE, San Diego, USA, pp. 177–184, 2000.
- [25] M. A. Horton, A. R. Newton. Method and Apparatus for Determining Position and Orientation of a Moveable Object Using Accelerometers, Patent 5615132, USA, March 1997.
- [26] M. Bousbia-Salah, M. Fezari. A navigation tool for blind people. *Innovations and Advanced Techniques in Computer and Information Sciences and Engineering*, T. Sobh, Ed., Netherlands: Springer, pp. 333–337, 2007.
- [27] M. Bousbia-Salah, M. Bettayeb, A. Larbi. A navigation aid for blind people. *Journal of Intelligent and Robotic Systems*, vol. 64, no. 3–4, pp. 387–400, 2011.
- [28] M. L. Anjum, J. Park, W. Hwang, H. I. Kwon, J. H. Kim, C. Lee, K. S. Kim, D. I. Cho. Sensor data fusion using unscented Kalman filter for accurate localization of mobile robots. In *Proceedings of International Conference on Control Automation and Systems (ICCAS)*, IEEE, Gyeonggido, Korea, pp. 947–952, 2010.
- [29] N. Houshangi, F. Azizi. Mobile robot position determination using data integration of odometry and gyroscope. In *Proceedings of 2006 World Automation Congress*, IEEE, Budapest, Hungary, pp. 1–8, 2006.
- [30] S. Julier, J. Uhlmann, H. F. Durrant-Whyte. A new method for the nonlinear transformation of means and covariances in filters and estimators. *IEEE Transactions on Automatic Control*, vol. 45, no. 3, pp. 477–482, 2000.
- [31] F. Azizi, N. Houshangi. Sensor integration for mobile robot position determination. In *Proceedings of IEEE International Conference on Systems, Man and Cybernetics*, IEEE, Washington, USA, pp. 1136–1140, 2003.
- [32] A. Sakai, Y. Tamura, Y. Kuroda. An efficient solution to 6dof localization using unscented Kalman filter for planetary rovers. In *Proceedings of IEEE/RSJ International Conference on Intelligent Robots and Systems*, IEEE, St. Louis, USA, pp. 4154–4159, 2009.
- [33] C. J. Sun, H. Y. Kuo, C. E. Lin. A sensor based indoor mobile localization and navigation using unscented Kalman filter. In *Proceedings of 2010 IEEE/ION Position Location and Navigation Symposium (PLANS)*, IEEE, Indian Wells, California, USA, pp. 327–331, 2010.
- [34] I. Arasaratnam, S. Haykin, T. R. Hurd. Cubature Kalman filtering for continuous-discrete systems: Theory and simulations. *IEEE Transactions on Signal Processing*, vol. 58, no. 10, pp. 4977–4993, 2010.

- [35] P. Closas, C. Fernyández-Prades. Bayesian nonlinear filters for direct position estimation. In *Proceedings of IEEE Aerospace Conference*, IEEE, Big Sky, USA, pp. 1–12, 2010.



**Derradji Nada** received the B.Sc. and M.Sc. degrees in electrical engineering from University of Bordj Bou Arreridj, Algeria in 2009 and 2011, respectively. He is currently Ph.D. degree candidate at Laboratory of Automatic and Signals Annaba (LASA), Department of Electronic Engineering, Badji Mokhtar Annaba University, Algeria.

His research interests include filtering, estimation, image compression and restoration, sensors and measurement.

E-mail: derradji.nada@univ-annaba.org

ORCID iD: 0000-0001-5336-2900



**Mounir Bousbia-Salah** received the B.Eng. degree in electronics from Annaba university, Algeria in 1984, the M.Sc. degree in electronics from Cardiff University, UK in 1988, and the Ph.D. degree in electronics from BADJI Mokhtar Annaba university, Algeria in 2004. He is a full professor and director of research with the Department of Electronic Engineering, BADJI Mokhtar Annaba University, Algeria. He is also head of research team in biomedical engineering with the Laboratory of Automatic and Signals of Annaba (LASA). He has been a reviewer with *IEEE Sensors Journal*, *Instrumentation Science and Technology*, *Measurement Science and Technology*, *Disability and Rehabilitation*, *Journal of Intelligent and Robotic Systems*, *Industrial Robot*, *Sensors and Transducers Journal*, *Journal of Electrical and Electronics Engineering Research* and many international

conferences. He is also member of the International Frequency Sensor Association and affiliated with IFAC. He has published more than 50 journal and conference papers and one book chapter.

His research interests include biomedical electronics, man-machine communication, sensors and control.

E-mail: bousbia.salah@univ-annaba.org (Corresponding author)

ORCID iD: 0000-0002-2611-9670



**Maamar Bettayeb** received the B.Sc., M.Sc., and Ph.D. degrees in electrical engineering from University of Southern California, USA in 1976, 1978 and 1981, respectively. He has been professor at University of Sharjah, UAE since August 2000. He also held the position of advisor to the Chancellor for Graduate Studies and Scientific Research for the years 2004/2006 and

director of Research and Studies Center for the Year 2005/2006 at University of Sharjah, UAE. He was associate editor of the *International Journal of Modeling, Identification and Control*. He is the leader of Intelligent Systems Research Group at University of Sharjah, UAE. He has published over 300 journal and conference papers and has over 1100 citations in recognition of his research contributions in the fields of control and signal processing. He has also supervised over 50 M.Sc. and Ph.D. students. He has been consulting for the Petrochemical Industries and has also been involved in various R&D funded projects in the areas of control and signal processing applications.

His research interests include  $H_\infty$  control, rational approximation, signal and image processing, process control, networked control systems, fractional dynamics and control, nonlinear estimation and filtering, software computing, wavelets, renewable energies and engineering education.

E-mail: maamar@sharjah.ac.ae